Factors Influencing Strain-Age Cracking in Inconel X-750

A study is undertaken to determine the mechanical response of an age-hardenable superalloy—Inconel X-750—to tensile loads in temperatures from 1000-1750° F to identify any microstructural changes that accompany deformation in this temperature range

BY A. W. DIX AND W. F. SAVAGE

ABSTRACT. The problem of cracking in precipitation hardenable high temperature alloys during postweld heat treatment has been studied by numerous investigators. However, in all the proposed theories, no attempt has been made to study the deformation modes operating in the temperature range where strain-age cracking occurs. Such information would seem vital to a complete understanding of the mechanism of postweld heat treatment cracking in this class of alloys. Therefore, this investigation was undertaken to determine the mechanical response of a relatively simple age-hardenable superalloy, Inconel X-750, to tensile loads in the temperature range of 1000–1750° F, and to identify any microstructural changes that accompany deformation in this temperature range.

The mechanical response to stress in the temperature range of 1000–1750° F was obtained from short-time tensile tests conducted at a series of loading rates ranging from 0.16–16.0 ipm. The fractured samples were then examined for any microstructural changes which accompanied the tensile deformation.

All testing was done in the RPI Gleeble, and the resultant microstructures were examined using both optical and transmission electron microscopy. Fracture morphology studies were also made using standard replication techniques supplemented by scanning electron microscopy.

The results of the short-time elevated temperature tensile tests revealed that the tensile ductility of Inconel X-750 loaded at rates ranging from 0.16–16.0 ipm exhibited a minimum in the vicinity of 1600° F. Both the testing temperature at which the minimum occurred and the ductility at this minimum increased as the strain rate increased. Failure in the temperature range where the minimum ductility occurred was found to be associated with grain boundary sliding.

The balance between the contribution of grain boundary sliding and transgranular slip to the overall deformation process appeared to control the ductility in the range 1000–1750° F, with an increase in the amount of grain boundary sliding causing a decrease in ductility. Grain boundary sliding was found to increase both as the strain rate was decreased and as the testing temperature was increased from 1000-1600° F. Recrystallization was observed to occur at 1700° F and was accompanied by an increase in ductility.

Although evidence was found that both fracturing of the carbides and separation at the carbide-matrix interface occurred as a result of plastic deformation, grain boundary carbides appeared to inhibit grain boundary sliding. No evidence was found of embrittlement due to either stress-induced or strain-induced precipitation of either γ' or carbides during the short-time elevated temperature tests.

Introduction

Advances in modern technology necessitate the use of materials exhibiting both high strength and corrosion resistance at elevated temperatures. Numerous precipitation hardenable nickel-base alloys have been developed to meet this need. However, the use of these materials is often limited because of failures which occur during postweld heat treatment. This type of failure is often referred to as strain-age cracking.

The proposed theories for strain-age cracking have been summarized by other authors.[1, 2] All theories were predicated on the theory that failure will occur when a stress of sufficient magnitude acts on a susceptible microstructure at an appropriate elevated temperature. The stresses contributing to failure have been suggested to include residual welding stresses, stresses due to localized thermal expansion, and aging contraction stresses. The precipitation of intergranular carbides has often been suggested as the cause of embrittlement in the aging temperature range. However, this embrittlement mechanism has become questionable in the light of recent investigations.[1-3]

Duvall and Owczarski[2] studied the fracture of Waspaloy and Inconel 718 using both stress-relaxation and tensile tests performed with the Gleeble. They reported that the cracking exhibited a "C-curve" type of time-temperature relationship with the minimum time for crack initiation occurring at 1600° F. Metallographic studies of weld heat-affected zones in Waspaloy failed to indicate any microstructural changes which would explain the embrittlement associated with postweld aging treatments. They concluded that the reduction in ductility during postweld heat treatment was the principal factor leading to failure.

Prager and co-workers[3-5] showed that the resistance of René 41 to cracking during postweld heat-treatment varied directly with the ductility in the vicinity of 1600° F. Short-time tensile tests showed that the ductility decreased with increasing temperature to a minimum at about 1600° F, and increased rapidly at higher testing temperatures. In addition, samples tested in air were found to have lower ductilities than samples tested in nitrogen, argon or vacuum.

The above authors concluded that hyperfine particles of γ' in the weld heat-affected zone establish the microstructure necessary for cracking

Table 1—Chemical Analysis of Inconel X-750, %

C	Mn	Fe	S	Si	Cu
0.03	0.51	6.65	0.007	0.30	0.08

Ni	Cr	Al	Ti	Cb & Ta
73.21	15.12	0.70	2.45	0.92

A. W. DIX is an Instructor and W. F. SAVAGE is Director of Welding Research, School of Engineering, Rensselaer Polytechnic Institute, Troy, N. Y.

Paper presented at the AWS 52nd Annual Meeting held in San Francisco, Calif., during April 26-29, 1971.

during postweld heat treatment of precipitation hardened nickel-base alloys. Dislocations generated by the thermal strains in welding can form pile-ups at grain boundaries and other barriers to their motion. Above about 1400° F, in oxygen containing environments, the grain boundaries are weakened by the absorption of oxygen and cracks initiate at the stress concentration ahead of the dislocation pile-ups.[3]

In all the proposed theories, no attempt has been made to study the deformation modes operating in the temperature range where strain-age cracking occurs. However, such information would seem vital to a complete understanding of the mechanism of post-weld heat treatment cracking in precipitation hardenable nickel-base alloys.

Objectives

The objectives of this investigation were:

1. To determine the mechanical response of Inconel X-750 to tensile loads in the temperature range from 1000-1750° F.
2. To identify and categorize any microstructural changes that accompany deformation in this temperature range.

Materials

The Inconel X-750 used in this investigation was prepared according to conventional mill practice and was supplied in the mill annealed condition as $^1/_{16}$ in. sheet. The chemical analysis of the as-received material is shown in Table 1. Before testing the samples were solution annealed at 2000° F for 2 hr and water quenched.

Experimental Procedure

Gleeble Tests

Specimens were sheared into $^1/_2$ × 3 in. blanks and machined into tensile specimens as shown in Fig. 1. Two 0.010 in. wires were precussion welded 0.4 in. apart, and symmetrically located relative to the specimen center to provide an identifiable gage length. To prevent any slippage in the jaws during testing, locking pins were inserted in the $^1/_4$ in. holes in the ends of specimens and butted against the holding grips.

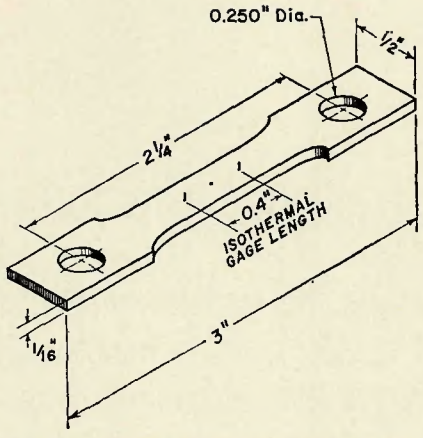

Fig. 1—Isometric representation of specimen geometry

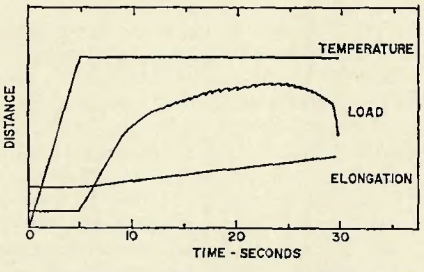

Fig. 2—Schematic representation of an oscillographic recording of an elevated temperature tensile test

The specimens were placed in an argon atmosphere chamber and heated to the selected testing temperatures in 5 sec at a constant rate. Upon reaching the desired temperature, the specimens were uniaxially loaded in tension at a constant crosshead velocity until failure occurred.* Two strain rates, 0.16 and 16.0 ipm, were used over a temperature range of 1000–1750° F. In addition, two temperatures, 1300 and 1600° F, were chosen to study the sensitivity of the alloy to intermediate values of strain rate.

Figure 2 is a schematic representation of a typical oscillographic recording of load, total elongation (i.e. platen motion), and temperature as a function of time. In addition the actual elongation in the 0.4 in. gage length, the fracture area, and the time to fracture were measured.

Fracture Studies

Both conventional and scanning electron microscopy were employed in studying the tensile fractures. Fracture morphology studies were made using both chromium-shadowed, acetate replication techniques, and scanning electron microscopy. Fracture initiation studies were made by straining prepolished specimens 0.100 in. (approximately 25%) at 1500° F in an argon atmosphere at 40 ipm. The deformed surface was then examined by scanning electron microscopy.

Metallographic Examination

Longitudinal sections of the fractured tensile specimens were prepared for examination by conventional metallographic techniques. In all cases etching was performed in a 10% aqueous solution of oxalic acid using 6 volts applied between the specimen and a stainless steel cathode.

Selected samples were prepared for transmission electron microscopy. The $^1/_{16}$ in. samples were first mechanically ground to a thickness of 4–7 mils. Samples were removed adjacent to the fracture surface and electro-

*The velocity of the crosshead will be hereafter referred to as "strain rate" to conserve words.

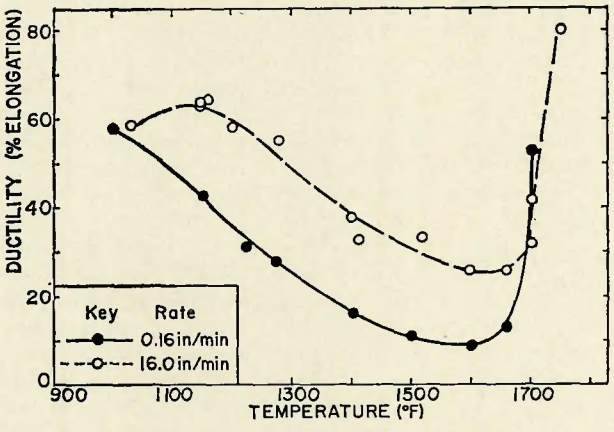

Fig. 3—Effect of testing temperature on ductility at two different strain rates

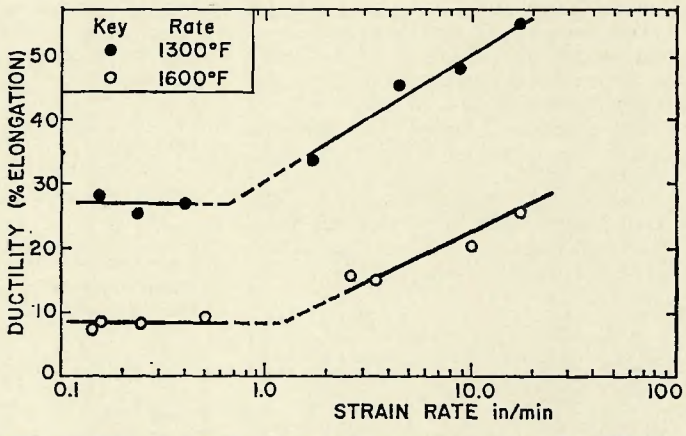

Fig. 4—Effect of strain rate and temperature on the ultimate tensile strength and yield stress

chemically thinned by the following two-stage technique:

1. An initial depression was created in the center of the sample by jet polishing with a solution consisting of 40 ml H_3PO_4, 35 ml H_2SO_4, and 25 ml H_2O using 35–60 ma at 130 volts d–c.

2. Final thinning was then performed in a solution consisting of 20% perchloric acid and 80% ethyl alcohol by maintaining 7.5 volts d–c between the specimen and two stainless steel cathodes located on opposite sides of the specimen until a fine pinhole developed in the original depression.

Results and Discussion

Mechanical Behavior

Tensile deformation in the temperature range of 1000–1660° F was accompanied by serrated yielding as shown schematically in Fig. 2. The actual number of serrations or load drops decreased sharply as the temperature was increased in this range. Samples tested above 1660° F did not exhibit this type of yielding. The number of load drops was also found to decrease as the strain rate was increased.

This behavior is similar to that found by Harding and Honeycombe[6] in austenitic steels containing Nb and Ti. They attributed the serrations to immobilization of dislocations caused by the precipitation of carbides along the dislocations. Owczarski[2] reported similar behavior in Waspaloy and Inconel 718, although serrated yielding was reported to occur over a limited temperature range.

Figure 3 shows the ductility as a function of testing temperature for Inconel X-750 in the temperature range of 1000–1750° F for two strain rates, 0.16 and 16.0 ipm. It should be recalled that these rates are actually the rates of motion of the platen, but can be considered to be proportional to the actual strain rates if one considers the deformation to have been confined to an isothermal gage section approximately 0.4 in. long.

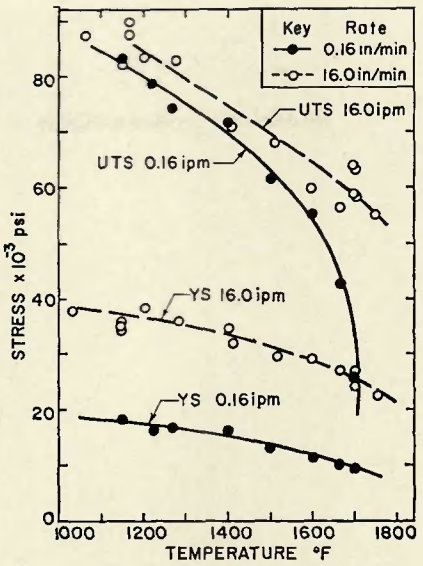

Fig. 5—Effect of strain rate on ductility at two different testing temperatures

The results shown in Fig. 3 indicate that Inconel X-750 exhibits the classical ductility minimum[7] for both strain rates. Note that the present elongation decreased from 56% at 1000° F to 9% at 1600° F for the slower strain rate, but showed a smaller decrease to 25% at 1600° F and 1660° F for a strain rate of 16 ipm. As the testing temperature was increased above the value where the ductility minimum occurred, the ductility increased rapidly for both strain rates.

Figure 4 shows the effect of strain rate and temperature on the yield stress and ultimate tensile strength in the temperature range of 1000–1750° F. The strain rate sensitivity of the yield stress is greater than the ultimate tensile strength except at testing temperatures exceeding 1600° F. Above 1600° F, the ultimate tensile strength decreases rapidly for the 0.16 ipm. strain rate and approaches the yield stress at temperatures above 1700° F.

The effect of strain rate on the ductility at 1300 and 1600° F is shown in Fig. 5. It should be recalled that 1600° F corresponds to the ductility minimum for a strain rate of 0.16 ipm, but is slightly below the minimum for 16.0 ipm. The change in slope of the curves in Fig. 5 indicates that a change in the deformation mechanism must occur within the range of strain rates studied. Attention is also called to the fact that the ductility at 1600° F for a strain rate of 16.0 ipm and that observed at 1300° F for strain rates less than 0.5 ipm are nearly identical.

In order to gain more knowledge concerning the mechanism causing the effects shown in Figs. 3–5, selected samples were prepared for examination by optical and transmission electron microscopy.

Metallographic Examination

Figure 6 is a photomicrograph taken at X100 of the solution annealed Inconel X-750 used in this investigation. The microconstituents present have been well documented[8] and consist of a gamma matrix containing $M_{23}C_6$, (Cb, Ta)C and Ti (CN) particles. Furthermore, since the alloy is relatively simple, only one additional constituent, namely gamma prime (γ'), forms during the aging treatment. Gamma prime, Ni_3 (Al, Ti), is formed in the temperature range of 1300–1600° F as a coherent precipitate. The shape of this γ' depends upon the previous thermal history,[9] being spherical if formed at low aging temperatures and cubic when formed by long exposures to high aging tem-

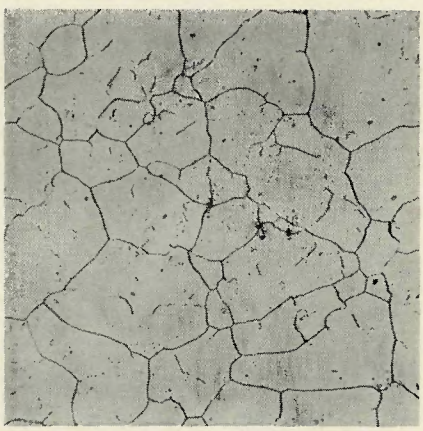

Fig. 6—Microstructure of Inconel X-750 after solution annealing for 2 hr at 2000° F. ×100 (reduced 35% on reproduction)

Fig. 7—Microstructure produced by heating to 1275° F and loading to failure at a rate of 16.0 ipm. ×100 (reduced 35% on reproduction)

Fig. 8—Microstructure produced by heating to 1270° F and loading to failure at a rate of 0.16 ipm. ×100 (reduced 35% on reproduction)

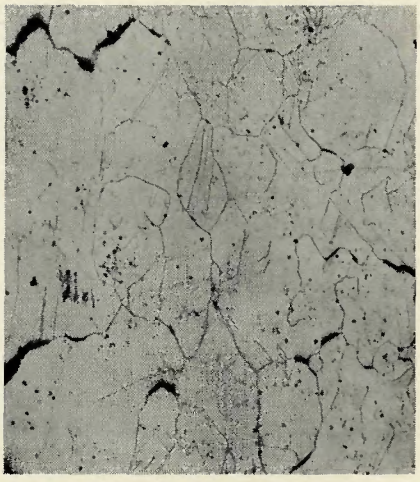

Fig. 9—Microstructure produced by heating to 1600° F and loading to failure at a rate of 16.0 ipm. ×100 (reduced 35% at reproduction)

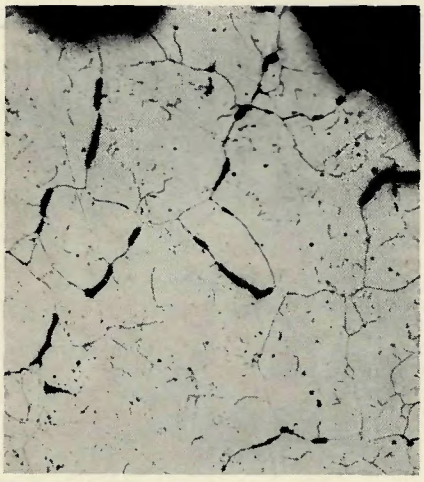

Fig. 10—Microstructure produced by heating to 1600° F and loading to failure at a rate of 0.16 ipm. ×100 (reduced 35% on reproduction)

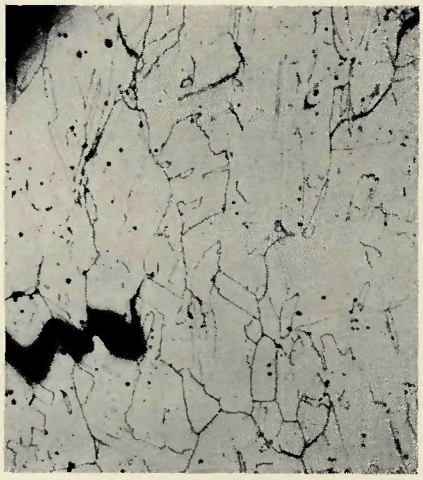

Fig. 11—Microstructure produced by heating to 1700° F and loading to failure at a rate of 16.0 ipm. ×100 (reduced 35% on reproduction)

peratures. The $M_{23}C_6$ carbides also form at high aging temperatures.

Figure 7 is a photomicrograph at X100 showing the structure formed by heating to 1275° F and loading to failure at a rate of 16.0 ipm. The microstructure is characteristic of a severely cold worked material, as indicated by the elongated grain structure and the tendency for the twins to become aligned with the direction of loading. This sample exhibited a total ductility of 56%. The fracture appeared to be predominantly transgranular.

A significant effect of strain rate on the deformation characteristics can be seen by comparing Figs. 7 and 8. The latter is a photomicrograph at X100 showing the structure formed by heating to 1270° F and loading at a rate of 0.16 ipm. The appearance of the microstructure indicates that both grain boundary sliding and transcrystalline slip occurred simultaneously. The former produces wedge shaped voids at grain boundary intersections,[10] while transgranular slip "bends" the normally straight sided annealing twins. This photomicrograph shows much less evidence of grain elongation and preferred orientation of the twins. This is consistent with the observed reduction in ductility as compared to the sample shown in Fig. 7 (29% vs. 56%).

Careful examination of the sample tested at 0.16 ipm revealed secondary cracking associated with carbide particles as may be seen in Fig. 12. This cracking is associated with both intragranular and intergranular carbides, indicating that deformation did occur by a combination of the two modes discussed above.

Cracking associated with the carbide phase was observed in all samples tested, although the severity of such cracking increased as the testing temperature decreased. The role of carbides in the fracture of high temperature alloys is reported to be strongly dependent upon their location and morphology. In alloys exhibiting ductile failure by void coalescence and growth, carbides have often been associated with crack initiation. In stress-rupture tests, blocky intergranular carbides are said to increase rupture life while discontinuous or cellular carbides are said to decrease rupture life.[11]

Figure 9 is a photomicrograph at X100 showing the structure formed by heating to 1600° F in 5 sec and loading at a rate of 16.0 ipm. Attention is drawn to the similarity between both the ductility and the microstructures of the specimens shown in Figs. 8 and 9. Both samples exhibit an elongation of 29% and show evidence of both grain boundary sliding and transgranular slip. However the sample tested at 1600° F and 16.0 ipm (Fig. 9) exhibits more intergranular

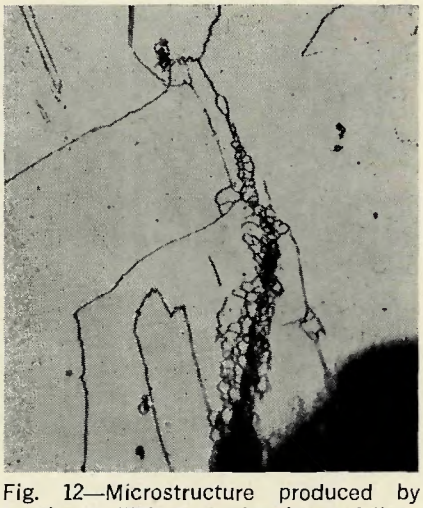

Fig. 12—Microstructure produced by heating to 1700° F and loading to failure at a rate of 16.0 ipm. ×500 (reduced 35% on reproduction)

Fig. 13—Microstructure produced by heating to 1700° F and loading to failure at a rate of 0.16 ipm. ×100 (reduced 35% on reproduction)

Fig. 14—Microstructure produced by heating to 1700° F and loading to failure at a rate of 0.16 ipm. ×500 (reduced 35% on reproduction)

cracking than the sample tested at 1270° F and 0.16 ipm (Fig. 8). The shorter time for grain boundary relaxation associated with the faster strain rate of 16.0 ipm apparently increased the likelihood of crack initiation at the highly stressed triple points. On the other hand, at the slower strain rate of 0.16 ipm more time is available for this relaxation and the cracking tendency appears to have decreased. The effect of temperature on grain boundary sliding at the slow strain rate is best illustrated by considering Fig. 10

Figure 10 is a photomicrograph at X100 of the structure formed by heating to the ductility minimum temperature of 1600° F and straining at a rate of 0.16 ipm. Not only does the elongation show a minimum of 9%, but also the amount of intergranular cracking is much greater than that shown in either of the two previous samples. Both wedge cracks formed at grain boundary intersections and secondary cracks located between the grain boundary triple points are evident in Fig. 10. The mechanism of formation of this second type of crack also necessitates grain boundary sliding.[12]

Attention is also drawn to the grain structure of the sample shown in Fig. 10. The grain boundaries etch much faster than the annealing twins, which are not as readily visible as in previous figures. When visible, however, the twin boundaries appear straight indicating that relatively little transgranular deformation has taken place. Also there is no evidence of preferred orientation of the grains which is further indication that grain boundary sliding is the controlling deformation mechanism for slow strain rates at 1600° F.

Figure 11 is a photomicrograph at X100 of the structure formed by heating to 1700° F and loading at a rate of 16.0 ipm. Attention is drawn to the similarity of this structure and the structures shown in Figs. 8 and 9. All three microstructures show evidence of both grain boundary sliding and transgranular deformation. Careful examination of Fig. 11, however, indicates one difference: recrystallization has occurred at a few grain boundaries and at the crack tips.

Figure 12 is a photomicrograph at X500 showing the start of this recrystallization. Small equiaxed recrystallized grains formed along the prior grain boundary appear to have hindered further growth of the existing crack. The result is an increase in the ductility from 25% elongation at 1600° F to 32% at 1700° F.

The structure formed by heating to 1700° F and loading at a rate of 0.16 ipm is shown in Fig. 13. This photomicrograph, taken at X100, shows that recrystallization has occurred in the regions extensively deformed by grain boundary sliding to a much greater extent than in the specimen tested at 16.0 ipm (Figs. 11 and 12). The new recrystallized grains appear to have hindered the propagation of the grain boundary cracks. Thus more plastic deformation is necessary to cause failure at 1700° F with a 0.16 ipm strain rate than with a 16.0 ipm rate. This increase in the total elongation to 53% elongates the grains and reorients the twins as may be seen in Fig. 13.

Figure 14 is a photomicrograph at X500 showing the "isolation" of cracks by regions of recrystallization. It is also of interest to note the tortuous appearance of the grain and twin boundaries in regions where no equiaxed recrystallized structure is present. This is attributed to strain induced migration of the boundaries through highly strained regions leaving behind a strain-free recrystallized structure.[13]

In summary, two deformation modes are operating in Inconel X-750 at elevated temperatures. These are grain boundary sliding and generalized transgranular slip. The relative importance of each mode is dependent upon temperature and strain rate.

At temperatures above 1000° F and at slow strain rates, neither deformation mode appears to predominate and substantial ductility results. As the deformation temperature is increased, grain boundary sliding tends to predominate over transgranular slip, causing a gradual decrease in ductility to a minimum near 1600° F. At temperatures above that where minimum ductility occurs, localized grain boundary deformation causes grain boundary migration and/or recrystallization and the ductility increases rapidly.

At strain rates greater than 1.0 ipm, the temperature at which grain boundary sliding begins to predominate and the temperature at which recrystallization starts both increase. This causes a slight increase in the temperature at which the minimum ductility occurs. Furthermore, the relative amount of transgranular slip is increased at the higher strain rates, thus explaining the improved ductility associated with changing the strain rate from 0.16–16.0 ipm.

Fracture Studies

From previous discussion, grain boundary sliding promotes intergranular fracture at elevated temperatures and the ductility decreases to a minimum near 1600° F. In order to study the fracture mode, chromium-shadowed acetate replicas were made of selected samples. All samples showed regions of dimpled fracture caused by void coalescence and growth. These dimples varied in both size and shape. In general, the size of the dimples decreased as the ductility diminished, while the dimples became more elongated as the testing temperature was increased up to the recrys-

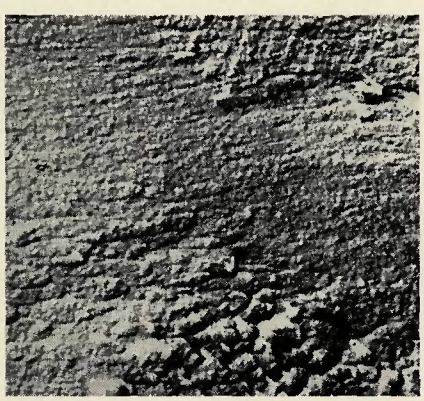

Fig. 15—Electron micrograph of the fracture surface of a specimen heated to 1600° F and loaded to failure at a rate of 16.0 ipm. ×4000 (reduced 28% on reproduction)

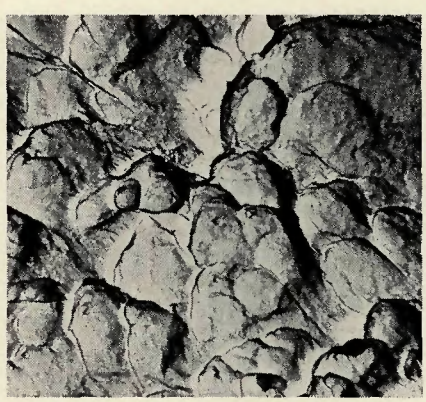

Fig. 16—Electron micrograph of the fracture surface of a specimen heated to 1275° F and loaded to failure at a rate of 16.0 ipm. ×4000 (reduced 28% on reproduction)

Fig. 17—Scanning electron micrograph of the fracture surfacing of a specimen heated to 1600° F and loaded to failure at a rate of 0.62 ipm. ×500 (reduced 40% on reproduction)

tallization temperature. In addition, many of the dimples were associated with second phase particles.

Figure 15 is an electron micrograph at X4000 of a sample heated to 1600° F and loaded at a rate of 16.0 ipm. This factograph shows both a region of grain boundary sliding devoid of dimples and a region exhibiting a fine dimpled structure. This dimple size should be compared with that revealed in Fig. 16, which shows the fracture surface of a sample heated at 1275° F and loaded at the same strain rate of 16.0 ipm. Note that the size of the dimples is much coarser in Fig. 16 than in Fig. 15. Note also that many of the dimples shown in Fig. 16 are associated with carbides.

Many fractographs showed marks caused by carbides on one fracture surface sliding over the mating surface. This would suggest that the presence of carbides on the grain boundaries should inhibit grain boundary sliding. The fact that some grain boundary carbides are beneficial in the prevention of grain boundary sliding is supported by Fig. 17. This figure is a scanning electron micrograph at X500 of the fracture surface of a sample tested at 1600° F at a strain rate of 0.62 ipm. Reference to Fig. 5 reveals that a change in strain rate from 0.16–0.62 ipm has no effect on the ductility at 1600° F. Therefore, it is assumed that this change in strain rate would not have altered the fracture mode at this temperature. Note that the two carbide particles (arrows) appear to interfere with further growth of the intergranular crack.

Evidence for both of the deformation modes previously discussed can be found in Fig. 18. This figure is a scanning electron micrograph at X1000 of the surface of a prepolished sample heated to 1500° F and strained 0.100 in. at a rate of 40.0 ipm. The slip lines visible in each of the grains indicate that an appreciable amount of transgranular deformation occurred. More important, however, is the evidence of grain boundary sliding. The height differences revealed at points A and B indicate that grain boundary sliding must have occurred even at this rapid rate of loading. Further evidence of grain boundary sliding is provided by the presence of two types of intergranular cracking—a wedge crack at a triple point at B and other voids located along the grain boundary near C.

Fig. 18—Scanning electron micrograph of the surface of a prepolished sample heated to 1500° F and strained 0.100 in. at a rate of 40 ipm. ×1000 (reduced 40% on reproduction)

Transmission Microscopy Studies

Transmission microscopy at magnifications up to X100,000 failed to reveal evidence of either γ' or carbide precipitation during short time tensile tests in the range 1000–1750° F. Thus, no support could be obtained for the hypothesis that precipitation phenomena occurring during the early stages of postweld heat-treatment cause localized embrittlement leading to strain-age cracking. Nonetheless the deformation associated with the tensile tests (or with stress relaxation during postweld heat treatments of welds) may well introduce additional nucleation sites for subsequent precipitation of γ' and/or carbides.

Conclusions

1. The tensile ductility of Inconel X-750 loaded at rates ranging from 0.16–16.0 ipm exhibited a minimum in the vicinity of 1600° F.

2. Both the testing temperature at which the minimum ductility occurs and the ductility at this minimum increase as the strain rate was increased.

3. Failure in the temperature range where the minimum ductility occurs was associated with grain boundary sliding.

4. Although evidence was found that both fracturing of the carbides and separation at the carbide-matrix interface occurred as a result of plastic deformation, grain boundary carbides appear to inhibit grain boundary sliding.

5. The balance between the contribution of grain boundary sliding and transgranular slip to the overall deformation process appears to control the ductility in the range 1000–1750° F, with an increase in the amount of grain boundary sliding causing a decrease in ductility. Grain boundary sliding was found to increase as the strain rate was decreased and as the testing temperature was increased from 1000–1600° F.

6. With the onset of recrystallization the ductility increased sharply at all strain rates.

7. No evidence was found of stress-induced or strain-induced precipitation of either γ' or carbides during the short-time elevated temperature tests.

Acknowledgement

The authors wish to express their gratitude to the American Welding and Manufacturing Company for providing the material used in this investigation.

References

1. Thompson, E. G., Nunez, S., and Prager, M., "Practical Solutions to Strain-Age Cracking of René 41," WELDING JOURNAL, 47 (7) Research Suppl. 299-s to 312-s (1968).

2. Duvall, D. S., and Owczarski, W. A., "Studies of Post-weld Heat-Treatment Cracking in Nickel-Base Alloys," *Ibid.*, 48 (1) Research Suppl., 10-s to 22-s (1969).

3. Prager, M., and Sines, G., "A Mechanism for Cracking During Postwelding Heat-Treatment of Nickel-Base Alloys," WRC Bulletin No. 150 (May 1970).

4. Frawley, R. W., and Prager, M., "Evaluating the Resistance of René 41 to Strain-Age Cracking," WRC Bulletin No. 150 (May 1970).

5. Carleton, J. B., and Prager, M., "Variables Influencing the Strain-Age Cracking and Mechanical Properties of René 41 and Related Alloys," WRC Bulletin No. 150 (May 1970).

6. Harding, H. J., and Honeycombe, R. W. K., "Effect of Stacking Fault Precipitation on the Mechanical Properties of Austenitic Steels," *Journal of the Iron and Steel Institute, 204* (3), pp. 259-267 (1966).

7. Rhines, F. N., and Wray, P. J., "Investigation of the Intermediate Temperature Ductility Minimum in Metals," *Trans. ASM, 54* (2), pp. 117-128 (1961).

8. ASTM Committee E-4 on Metallography, "Electron Microstructure of Precipitation-Hardenable Austenitic and Nickel-Base Alloys," Symposium in Advances in Electron-Metallography, ASTM STP No. 262, Am. Soc. Testing Mat's., pg. 3, (1959).

9. Bigelow, W. C., Amy, J. A., Corey, C. L., and Freeman, J. W., "An Electron Metallographic Study of the Precipitation Hardening Process in Commercial Nickel-Base Alloys," Symposium in Advances in Electron Metallography, ASTM STP No. 245, Am. Soc. Testing Mat's., pg. 73 (1958).

10. Chen, C. W., and Grant, N. J., *Trans AIME, 206*, p. 169, (1956).

11. Sullivan, C. P., "A Review of Some Microstructural Aspects of Fracture in Crystalline Materials," WRC Bulletin No. 122 (May 1967).

12. Chen, C. W. and Macklin, E. S., "On a Mechanism of High Temperature Intercrystalline Cracking," *Trans. AIME*, Vol. 209, pg. 829 (1957).

13. Shewmon, P. G., "Transformations in Metals," pg. 98, McGraw-Hill Book Co., New York (1969).

Authors . . . See page 401 in this issue of the WELDING JOURNAL concerning the presentation of technical papers at the AWS 53rd Annual Meeting.